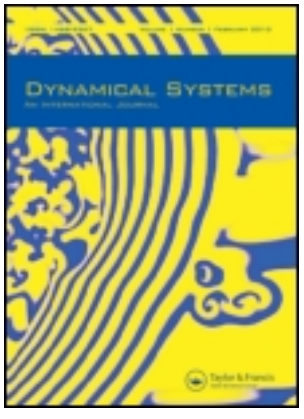

Dynamical Systems: An International Journal

Publication details, including instructions for authors and subscription information:
http://www.tandfonline.com/loi/cdss20

Switching near a network of rotating nodes

Manuela A.D. Aguiar [a], Isabel S. Labouriau [b] & Alexandre A.P. Rodrigues [b]

[a] Faculdade de Economia, Centro de Matemática, Universidade do Porto, Rua Dr. Roberto Frias, Porto 4200-464, Portugal

[b] Faculdade de Ciências, Centro de Matemática, Universidade do Porto, Rua do Campo Alegre 687, Porto 4169-007, Portugal

Version of record first published: 24 Sep 2009.

To cite this article: Manuela A.D. Aguiar, Isabel S. Labouriau & Alexandre A.P. Rodrigues (2010): Switching near a network of rotating nodes, Dynamical Systems: An International Journal, 25:1, 75-95

To link to this article: http://dx.doi.org/10.1080/14689360903252119

Dynamical Systems
Vol. 25, No. 1, March 2010, 75–95

Switching near a network of rotating nodes

Manuela A.D. Aguiar[a], Isabel S. Labouriau[b] and Alexandre A.P. Rodrigues[b]*

[a]*Faculdade de Economia, Centro de Matemática, Universidade do Porto, Rua Dr. Roberto Frias, Porto 4200-464, Portugal;* [b]*Faculdade de Ciências, Centro de Matemática, Universidade do Porto, Rua do Campo Alegre 687, Porto 4169–007, Portugal*

(*Received 7 November 2008; final version received 4 August 2009*)

We study the dynamics of a $\mathbf{Z}_2 \oplus \mathbf{Z}_2$-equivariant vector field in the neighbourhood of a heteroclinic network with a periodic trajectory and symmetric equilibria. We assume that around each equilibrium the linearization of the vector field has non-real eigenvalues. Trajectories starting near each node of the network turn around in space either following the periodic trajectory or due to the complex eigenvalues near the equilibria. Thus, in a network with rotating nodes, the rotations combine with transverse intersections of two-dimensional invariant manifolds to create switching near the network; close to the network, there are trajectories that visit neighbourhoods of the saddles following all the heteroclinic connections of the network in any given order. Our results are motivated by an example where switching was observed numerically by forced symmetry breaking of an asymptotically stable network with $\mathbf{O}(2)$ symmetry.

Keywords: heteroclinic network; switching; vector fields; symmetry breaking; shadowing

2000 Mathematics Subject Classifications: primary: 37G30; secondary: 37C10, 34C37, 37C29, 34C28, 37C80

1. Introduction

Heteroclinic connections and networks are a common feature of symmetric differential equations, and persist under perturbations that preserve the symmetry. We start with an asymptotically stable network with rotational symmetry. A perturbation that breaks part of the symmetry splits a two-dimensional connection into a pair of one-dimensional ones. The new network is no longer asymptotically stable, nearby trajectories follow the network around in a complex way that we call switching.

By a heteroclinic network we mean a connected flow-invariant set that is the union of heteroclinic cycles. In the present case, it is the orbit under the symmetry group $\mathbf{Z}_2 \oplus \mathbf{Z}_2$ of a heteroclinic cycle. These networks are often called heteroclinic cycles in the literature. Heteroclinic cycles and networks are known to occur persistently in the settings of symmetry [1,2], coupled cell systems (with and without symmetry) [3,4] and population dynamics [5–8]. They are induced by the existence of flow-invariant subspaces that correspond, respectively, to fixed point subspaces, synchrony subspaces and coordinate axes and hyperplanes.

*Corresponding author. Email: alexandre.rodrigues@fc.up.pt

ISSN 1468–9367 print/ISSN 1468–9375 online

DOI: 10.1080/14689360903252119
http://www.informaworld.com

It is worthwhile describing the general properties that entail switching, so the results may be applied to examples in other contexts. We study the dynamics near a network where all cycles have a common node that is a closed trajectory. We prove that there are trajectories near the network that follow its cycles in any desired order. Trajectories that go near the periodic orbit may switch to any heteroclinic cycle, return and switch again.

Several numerical reports on complicated dynamics near heteroclinic networks of equilibria and of equilibria and periodic trajectories that include random visits to the nodes of the network in any possible order exist in the literature [1,9–11].

This type of behaviour is not possible around asymptotically stable heteroclinic networks whose connections are contained in invariant subspaces. Each cycle in the network cannot be asymptotically stable but it may have strong attractivity properties [12,13] so that each nearby trajectory outside the invariant subspaces will tend to one of the cycles in the network.

Different forms of switching have been described in several contexts. Networks where all the nodes are equilibria have been studied by Postlethwaite and Dawes [14] who found trajectories that follow three cycles in a network sequentially, both regularly and irregularly; by Kirk and Silber [15] near a network with two cycles who found nearby trajectories that switch in one direction. Persistent random switching is found by Guckenheimer and Worfolk [9] and Aguiar *et al.* [16]; noise induced switching in Armbruster *et al.* [10].

A similar problem to ours, where a network involves equilibria and a periodic trajectory, appears in the heteroclinic model of the geodynamo derived in Melbourne *et al.* [17]. Starting with a model with $\mathbf{Z}_2 \oplus \mathbf{Z}_2 \oplus \mathbf{SO}(2)$ symmetry, they perturb the model so the only remaining symmetry is $-Id$. For the perturbed model, they establish switching numerically in terms of reversals and excursions.

This has motivated Kirk and Rucklidge [18] to ask whether switching would be observed when all the symmetries are broken. First they analyse partially broken symmetries in two different ways: when only the $\mathbf{SO}(2)$ symmetry remains they find a weak form of switching, where trajectories starting near one equilibrium may visit the neighbourhood of another but not return to the first one; for the $\mathbf{Z}_2 \oplus \mathbf{Z}_2$-symmetric case they find attracting periodic trajectories and no switching. Then they argue that when all symmetries are broken and the network is destroyed, switching will not take place arbitrarily close to $\mathbf{Z}_2 \oplus \mathbf{Z}_2$-symmetric problems because of barriers formed by invariant manifolds. They describe a scenario where switching may arise, if the symmetry-breaking terms are larger than a threshold value. They propose a mechanism for switching arising from the right combination of homoclinic tangencies between the stable and unstable manifolds of a periodic orbit and specific heteroclinic tangencies between stable and unstable manifolds of the equilibria.

Here we analyse equations with a symmetry group $\mathbf{Z}_2 \oplus \mathbf{Z}_2$, a subgroup of that considered by Melbourne *et al.* [17] but not acting in the same way as in Kirk and Rucklidge [18]: each $\boldsymbol{Z}_2$ in our setting contains a rotation by π that fixes a plane. A discussion of how our results compare with those of [18] and [17] appears at the end of this article in Section 9.

Under generic hypotheses for this symmetry, we prove a strong form of switching, the existence of trajectories that visit neighbourhoods of any sequence of nodes of the network in any order that is compatible with the network connections.

The conditions needed for switching are stated in Section 3 preceded by definitions and preliminary results in Section 2.

In Section 4, we present an example of a $\mathbf{Z}_2 \oplus \mathbf{Z}_2$-equivariant family of ordinary differential equations having a network of rotating nodes and some simulations (see Figures 3 and 4). When one of the parameters is set to zero, the equations are $\mathbf{Z}_2 \oplus \mathbf{Z}_2 \oplus \mathbf{SO}(2)$-symmetric and the network is asymptotically stable. Switching occurs for all small non-zero values of this symmetry-breaking parameter.

We linearize the flow around the invariant saddles in Section 5, obtaining isolating blocks around each node of the network. This section is mostly concerned with introducing the notation for the proof of switching that occupies the rest of the article.

The goal of this article is to prove switching in the neighbourhood of a heteroclinic network that consists of four symmetric copies of a heteroclinic cycle

$$\mathbf{C} \to \mathbf{v} \to \mathbf{w} \to \mathbf{C}$$

where $\mathbf{C}$ is a closed trajectory invariant under the symmetries and $\mathbf{v}$ and $\mathbf{w}$ are equilibria. The connection $\mathbf{v} \to \mathbf{w}$ is one-dimensional and takes place inside a fixed-point subspace, the other connections are transverse intersections of two-dimensional invariant manifolds. The trajectory $\mathbf{C}$ has real Floquet multipliers and two-dimensional stable and unstable manifolds; the linearization of the flow near $\mathbf{v}$ has a pair of complex eigenvalues with negative real part and one real positive eigenvalue; the linearization of the flow near $\mathbf{w}$ has one real negative eigenvalue and a pair of complex eigenvalues with positive real part (see Figures 1 and 2).

In Section 6, we obtain a geometrical description of the way the flow transforms a curve of initial conditions lying across the stable manifold of each node. The curve is wrapped around the isolating block of the next node, accumulating on its unstable manifold and in particular on the next connection. Thus, points on a line across the stable manifold of $\mathbf{v}$ will be mapped into a helix accumulating on the unstable manifold of $\mathbf{w}$ that will cross the transverse stable manifold of $\mathbf{C}$ infinitely many times. Similarly, points on a line across the stable manifold of $\mathbf{C}$ will be mapped into a helix accumulating on its unstable manifold and thus will cross the transverse stable manifold of $\mathbf{v}$ infinitely many times.

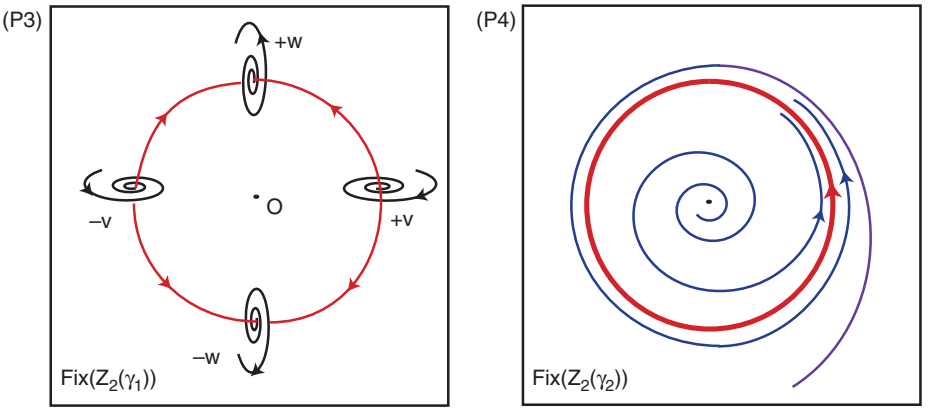

Figure 1. Dynamics near a heteroclinic network of rotating nodes. Left: dynamics around the plane Fix($\mathbf{Z}_2(\gamma_1)$) illustrating property (P3); Right: dynamics in the plane Fix($\mathbf{Z}_2(\gamma_2)$) illustrating property (P4).

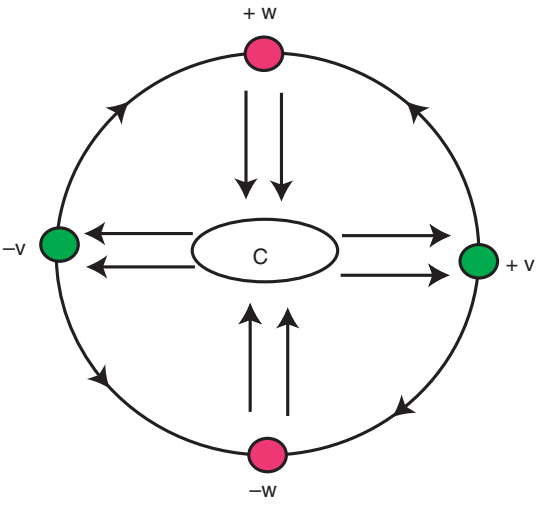

Figure 2. Schematic description of a heteroclinic network of rotating nodes satisfying (P1–P5). Each arrow represents a one-dimensional heteroclinic connection. There is one one-dimensional heteroclinic connection from each equilibrium $\pm\mathbf{v}$ to each equilibrium $\pm\mathbf{w}$(P3). There are two one-dimensional heteroclinic connections involving each equilibrium and the periodic trajectory $\mathbf{C}$ (P5).

The geometrical setting is explored in Section 7 to obtain intervals on the curve of initial conditions that are mapped by the flow into curves near the next node in a position similar to the first one. This allows us to establish the recurrence needed for switching in Section 8. For any sequence of nodes like

$$+\mathbf{v} \to -\mathbf{w} \to \mathbf{C} \to -\mathbf{v} \to -\mathbf{w} \to \mathbf{C} \to +\mathbf{v} \to +\mathbf{w} \to \mathbf{C} \to +\mathbf{v} \to \cdots$$

we find trajectories that visit neighbourhoods of these nodes in the same sequence.

We end the article with a discussion (Section 9) of the results obtained and of related results in the literature.

2. Preliminaries

Let f be a smooth vector field on $\mathbf{R}^n$ with flow given by the unique solution $x(t) = \varphi(t, x_0) \in \mathbf{R}^n$ of

$$\dot{x} = f(x), \quad x(0) = x_0. \tag{1}$$

If A is a compact invariant set for the flow of f, we say, following Field [1], that A is an *invariant saddle* if

$$A \subseteq \overline{W^s(A)\backslash A} \quad \text{and} \quad A \subseteq \overline{W^u(A)\backslash A},$$

where $\overline{A}$ is the closure of A. In this article all the saddles are hyperbolic.

Given two invariant saddles A and B, an m-dimensional *heteroclinic connection* from A to B, denoted $[A \to B]$, is an m-dimensional connected flow-invariant manifold contained in $W^u(A) \cap W^s(B)$. There may be more than one connection from A to B.

Let $\mathcal{S}=\{A_j: j\in\{1,\ldots,k\}\}$ be a finite ordered set of mutually disjoint invariant saddles. Following Field [1], we say that there is a *heteroclinic cycle* associated with $\mathcal{S}$ if

$$\forall j\in\{1,\ldots,k\},\quad W^u(A_j)\cap W^s(A_{j+1})\neq\emptyset \pmod k.$$

We refer to the saddles defining the heteroclinic cycle as *nodes*.

A *heteroclinic network* is a finite connected union of heteroclinic cycles.

Let Γ be a compact Lie group acting linearly on $\mathbf{R}^n$. The vector field f is Γ-equivariant if for all $\gamma\in\Gamma$ and $x\in\mathbf{R}^n$, we have $f(\gamma x)=\gamma f(x)$. In this case $\gamma\in\Gamma$ is said to be a symmetry of f. We refer the reader to Golubitsky *et al.* [19] for more information on differential equations with symmetry.

The Γ-*orbit* of $x_0\in\mathbf{R}^n$ is the set $\Gamma(x_0)=\{\gamma x_0,\gamma\in\Gamma\}$ that is invariant under the flow of Γ-equivariant vector fields f. In particular, if x_0 is an equilibrium of (1), so are the elements in its Γ-orbit.

The *isotropy subgroup* of $x_0\in\mathbf{R}^n$ is $\Gamma_{x_0}=\{\gamma\in\Gamma,\gamma x_0=x_0\}$. For an isotropy subgroup Σ of Γ, its *fixed-point subspace* is

$$\mathrm{Fix}(\Sigma)=\{x\in\mathbf{R}^n:\forall\gamma\in\Sigma,\gamma x=x\}.$$

Fixed-point subspaces are the reason for the robustness of heteroclinic cycles and networks in symmetric dynamics: if f is Γ-equivariant then $\mathrm{Fix}(\Sigma)$ is flow-invariant, thus connections occurring inside these spaces persist under perturbations that preserve the symmetry.

For a heteroclinic network Σ with node set $\mathcal{A}$, a *path of order* k, on Σ is a finite sequence $s^k=(c_j)_{j\in\{1,\ldots,k\}}$ of connections $c_j=[A_j\to B_j]$ in Σ such that $A_j,B_j\in\mathcal{A}$ and $B_j=A_{j+1}$ i.e. $c_j=[A_j\to A_{j+1}]$. For an infinite path, take $j\in\mathbf{N}$.

Let N_Σ be a neighbourhood of the network Σ and let U_A be a neighbourhood of each node A in Σ. For each heteroclinic connection in Σ, consider a point p on it and a small neighbourhood V of p. We are assuming that the neighbourhoods of the nodes are pairwise disjoint, as well for those of points in connections.

Given neighbourhoods as above, the point q, or its trajectory $\varphi(t)$, *follows* the finite path $s^k=(c_j)_{j\in\{1,\ldots,k\}}$ of order k, if there exist two monotonically increasing sequences of times $(t_i)_{i\in\{1,\ldots,k+1\}}$ and $(z_i)_{i\in\{1,\ldots,k\}}$ such that for all $i\in\{1,\ldots,k\}$, we have $t_i<z_i<t_{i+1}$ and:

(1) $\varphi(t)\subset N_\Sigma$ for all $t\in(t_1,t_{k+1})$;
(2) $\varphi(t_i)\in U_{A_i}$ and $\varphi(z_i)\in V_i$ and
(3) for all $t\in(z_i,z_{i+1})$, $\varphi(t)$ does not visit the neighbourhood of any other node except that of A_{i+1}.

There is *finite switching* near Σ if for each finite path there is a trajectory that follows it. Analogously, we define *infinite* switching near Σ by requiring that each infinite path is followed by a trajectory.

An infinite path on Σ may also be seen as a pseudo-orbit of $\dot{x}=f(x)$, with infinitely many discontinuities. Switching near Σ means that these infinite pseudo-orbits can be shadowed.

3. A network of rotating nodes

Our object of study is the dynamics around a special type of heteroclinic network (see Figure 2) for which we give a rigorous description here. The network lies in a

topological three-sphere and one of its nodes is a closed trajectory with real Floquet multipliers and two-dimensional stable and unstable manifolds. Near this node, the flow rotates following the closed trajectory. The other nodes are equilibria with a pair of non-real eigenvalues. Thus the local dynamics rotates around each node.

Specifically, we study a smooth vector field f on $\mathbf{R}^4$ with the following properties:

(P1) The vector field f is equivariant under $\Gamma \cong \mathbf{Z}_2 \oplus \mathbf{Z}_2$ acting linearly on $\mathbf{R}^4$ with generators γ_1 and γ_2 and with two transverse two-dimensional fixed-point subspaces. In particular, the origin is an equilibrium.

(P2) There is a three-dimensional flow-invariant manifold $\mathbf{S}^3$ diffeomorphic to a sphere that attracts all the trajectories except the origin. For simplicity, we assume this manifold to be the unit sphere.

By (P1–P2) there are two flow-invariant circles

$$\mathbf{C}_1 = \mathbf{S}^3 \cap \mathrm{Fix}(\mathbf{Z}_2(\gamma_1)) \quad \text{and} \quad \mathbf{C} = \mathbf{S}^3 \cap \mathrm{Fix}(\mathbf{Z}_2(\gamma_2)).$$

(P3) On $\mathbf{C}_1$ there are exactly four equilibria that will be denoted by $+\mathbf{v}$, $+\mathbf{w}$, $-\mathbf{v} = \gamma_2 \cdot \mathbf{v}$, $-\mathbf{w} = \gamma_2 \cdot \mathbf{w}$. Moreover, the eigenvalues of df restricted to $T\mathbf{S}^3$ are

- $-C_v \pm i$ and E_v with $C_v \neq E_v > 0$, at $\pm\mathbf{v}$;
- $E_w \pm i$ and $-C_w$ with $C_w \neq E_w > 0$, at $\pm\mathbf{w}$.

In $\mathrm{Fix}(\mathbf{Z}_2(\gamma_1))$ the equilibria $\pm\mathbf{v}$ are saddles and $\pm\mathbf{w}$ are sinks with connections in $\mathbf{C}_1$ from $\pm\mathbf{v}$ to $\pm\mathbf{w}$. These connections are persistent under perturbations that preserve the γ_1-symmetry (see Figure 1).

(P4) In the invariant plane $\mathrm{Fix}(\mathbf{Z}_2(\gamma_2))$ the only equilibrium is the origin and it is an unstable focus.

Thus $\mathbf{C}$ is a closed trajectory and, from (P2), this trajectory is a sink in $\mathrm{Fix}(\mathbf{Z}_2(\gamma_2))$ (see Figure 1). Since $\mathbf{C}$ is contained in the flow-invariant plane $\mathrm{Fix}(\mathbf{Z}_2(\gamma_2))$, its Floquet multipliers are real.

(P5) The periodic trajectory $\mathbf{C}$ is hyperbolic and, in $\mathbf{S}^3$, $\dim W^u(\mathbf{C}) = \dim W^s(\mathbf{C}) = 2$. Moreover, there are connections $[\mathbf{C} \to +\mathbf{v}]$ and $[+\mathbf{w} \to \mathbf{C}]$ satisfying:

$$W^u(\mathbf{C}) \pitchfork W^s(+\mathbf{v}) \quad \text{and} \quad W^u(+\mathbf{w}) \pitchfork W^s(\mathbf{C}).$$

These intersections are one-dimensional and consist of one pair of γ_1-related trajectories.

From the γ_2-symmetry, we obtain a pair of γ_1-related one-dimensional connections in $W^u(\mathbf{C}) \pitchfork W^s(-\mathbf{v})$ and in $W^u(-\mathbf{w}) \pitchfork W^s(\mathbf{C})$. It follows that there is a heteroclinic network Σ involving the saddles $\pm\mathbf{v}$, $\pm\mathbf{w}$ and $\mathbf{C}$ (see Figure 2). Such a network Σ is what we call a *network of rotating nodes*. This article shows switching near this network.

The symmetry γ_1 and its flow-invariant fixed point subspace ensure the persistence of the connections $[\pm\mathbf{v} \to \pm\mathbf{w}]$. The other symmetry γ_2 is not essential for the existence of a robust network with these properties but it makes them more natural as illustrated by the example in Section 4. The same is true for the existence of the invariant three-sphere. In Section 9, we discuss variants of these hypotheses for which switching may be proved in the same way.

4. Example

Our study was initially motivated by the following example constructed in Aguiar [20], using the methods of [21]. This is an ordinary differential equation in $\mathbf{R}^4$ given by

$$\begin{cases} \dot{x}_1 = x_1\big(\alpha_1 + \alpha_2 r_1^2 + \alpha_3 x_3^2 + \alpha_4 x_4^2 + \alpha_5(x_3^4 - r_1^2 x_4^2)\big) - x_2 \\ \dot{x}_2 = x_2\big(\alpha_1 + \alpha_2 r_1^2 + \alpha_3 x_3^2 + \alpha_4 x_4^2 + \alpha_5(x_3^4 - r_1^2 x_4^2)\big) + x_1 \\ \dot{x}_3 = x_3\big(\alpha_1 + \alpha_2 x_3^2 + \alpha_3 x_4^2 + \alpha_4 r_1^2 + \alpha_5(x_4^4 - r_1^2 x_3^2)\big) + \xi h_1(x) \\ \dot{x}_4 = x_4\big(\alpha_1 + \alpha_2 x_4^2 + \alpha_3 r_1^2 + \alpha_4 x_3^2 + \alpha_5(r_1^4 - x_3^2 x_4^2)\big) - \xi h_2(x) \end{cases}$$

where $x = (x_1, x_2, x_3, x_4) \in \mathbf{R}^4$, $r_1^2 = x_1^2 + x_2^2$ and

$$h_1(x) = \big[\alpha_1 + 3\alpha_2(x_1^2 + x_2^2)\big]x_1x_2x_4 \quad \text{and} \quad h_2(x) = \big[\alpha_1 + 3\alpha_2(x_1^2 + x_2^2)\big]x_1x_2x_3.$$

The symmetries of the equation are changes of sign of pairs of coordinates:

$$\gamma_1(x) = (-x_1, -x_2, x_3, x_4) \quad \gamma_2(x) = (x_1, x_2, -x_3, -x_4).$$

Figures 3 and 4 show a trajectory of this equation. In [20] it is proved that, for parameter values such that

$$\alpha_1 > 0, \quad \alpha_3 + \alpha_4 = 2\alpha_2, \quad \alpha_3 < \alpha_2 < \alpha_4 < 0$$
$$\alpha_2(\alpha_3 - \alpha_4) + \alpha_1\alpha_5 > 0$$

and if $\xi \geq 0$ is such that

$$\xi < \frac{-\alpha_2\alpha_3 + \alpha_2\alpha_4 + \alpha_1\alpha_5}{2\alpha_1\alpha_2} \quad \text{and} \quad \xi^2 < \frac{(\alpha_4 - \alpha_3)(2\alpha_1\alpha_5 - \alpha_2\alpha_3 + \alpha_2\alpha_4)}{4\alpha_1^2\alpha_2},$$

then its dynamics satisfies (P1–P4) as we proceed to explain.

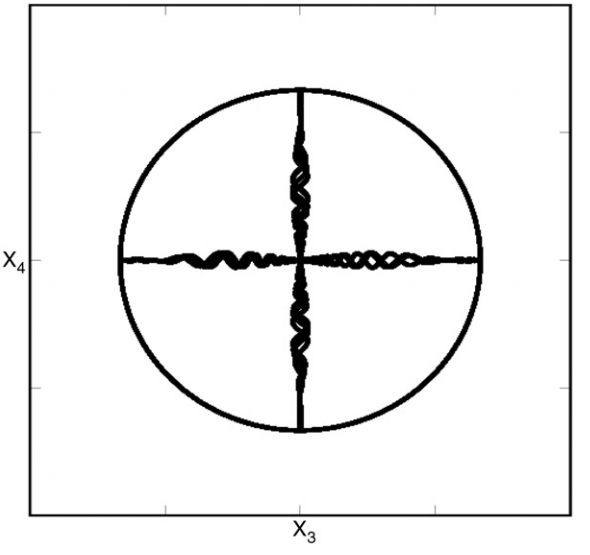

Figure 3. Switching trajectory on the example in Section 4: projection into the (x_3, x_4)-plane of the trajectory with initial condition $(0.001, 0.001, 0.001, 1)$, with $\alpha_1 = 0.33333333$, $\alpha_2 = -0.33333333$, $\alpha_3 = -0.5$, $\alpha_4 = -0.16666667$, $\alpha_5 = -0.05$ and $\xi = -1$.

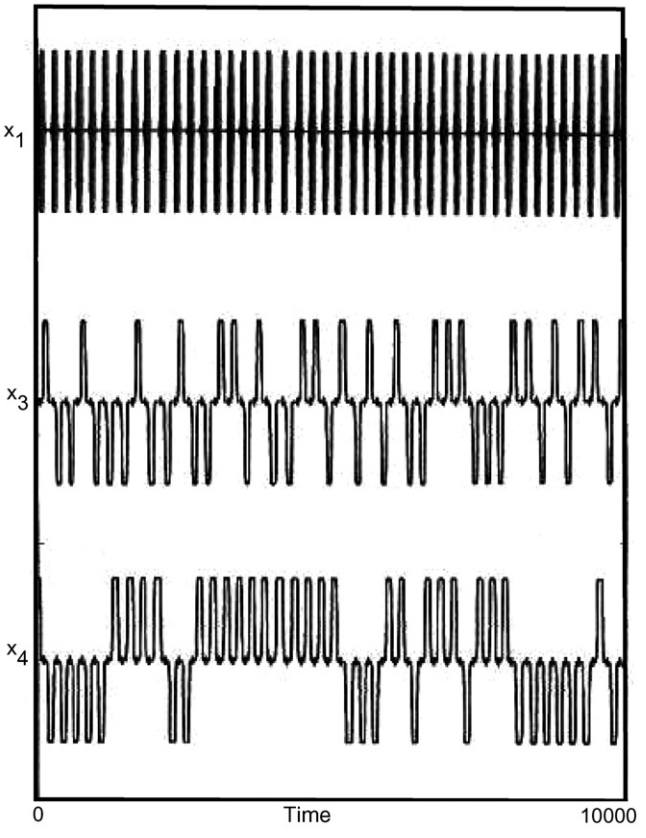

Figure 4. Switching trajectory on the example in Section 4: time series for x_1, x_3 and x_4 for a trajectory with initial condition $(0.001, 0.001, 0.001, 1)$, with $\alpha_1 = 0.33333333$, $\alpha_2 = -0.33333333$, $\alpha_3 = -0.5$, $\alpha_4 = -0.16666667$, $\alpha_5 = -0.05$ (same as Figure 3). The variable x_1 shows visits to the limit cycle, x_3 shows alternate visits to $\pm\mathbf{v}$ and x_4 shows visits to $\pm\mathbf{w}$.

For $\xi = 0$, the equation has more symmetry, like the model in Melbourne *et al.* [17]: it is equivariant under the group $\mathbf{Z}_2 \oplus \mathbf{Z}_2 \oplus \mathbf{SO}(2)$, generated by

$$\kappa_\varphi(x) = (x_1 \cos(\varphi) - x_2 \sin(\varphi), x_1 \sin(\varphi) + x_2 \cos(\varphi), x_3, x_4)$$
$$\kappa_2(x) = (x_1, x_2, -x_3, x_4) \quad \kappa_3(x) = (x_1, x_2, x_3, -x_4).$$

When $\xi = 0$, the three-dimensional sphere $\mathbf{S}^3_r$ of radius $r = \sqrt{\frac{-\alpha_1}{\alpha_2}}$ is flow-invariant and globally attracting. The equilibria $\pm\mathbf{v}$ (respectively $\pm\mathbf{w}$) lie at the intersection of $\mathbf{S}^3_r$ with the x_3-axis (respectively x_4-axis) fixed by the subgroup generated by κ_φ and κ_3 (respectively κ_φ and κ_2). The closed trajectory $\mathbf{C}$ is the intersection of $\mathbf{S}^3_r$ with the plane fixed by the subgroup generated by κ_2 and κ_3. A direct computation of the eigenvalues and eigenvectors shows that the closed trajectory and the equilibria form a network where the two-dimensional unstable (respectively stable) manifold of $\mathbf{C}$ coincides with the two-dimensional stable (respectively unstable) manifold of $\pm\mathbf{v}$ (respectively $\pm\mathbf{w}$). Since all the heteroclinic connections are contained in fixed point subspaces, there is no switching. Moreover, it can be shown (see [20]) that the network is asymptotically stable by the criteria of Krupa and Melbourne [22,23].

For $\xi > 0$, the $\mathbf{SO}(2)$ symmetry is broken and so are the two-dimensional connections. The only symmetries remaining are $\gamma_1 = \kappa_\pi$ and $\gamma_2 = \kappa_2\kappa_3$. The symmetry-breaking term $(0, 0, h_1(x), h_2(x))$ is tangent to the invariant sphere so it is still flow-invariant and properties (P1) and (P2) hold. The perturbation maintains the flow-invariance of the line that is fixed by κ_π and κ_2 (respectively κ_π and κ_3), the equilibria and the periodic trajectory are preserved together with their stability, and properties (P3–P4) hold. Using Melnikov's method, Aguiar [20] proved that the two-dimensional manifolds of the periodic trajectory and of the saddle-foci intersect transversely. Hence property (P5) holds. It follows from Theorem 7 that there is switching near this network as suggested by the trajectories like that of Figures 3 and 4.

5. Local dynamics near the saddles

Here and in the next two sections, we define the setup for the proof of switching near the network. This section contains mostly notation and coordinates used in the rest of the article.

We restrict our study to $\mathbf{S}^3$ since this is a compact and flow-invariant manifold that captures all the dynamics. When we refer to the stable/unstable manifold of an invariant saddle, we mean the local stable/unstable manifold of that saddle.

We use Samovol's theorem to linearize the flow around each saddle – equilibrium or closed trajectory. We then introduce local cylindrical coordinates and define a neighbourhood with boundary transverse to the linearized flow. For each saddle, we obtain the expression of the local map that sends points in the boundary where the flow goes in, into points in the boundary where it goes out. These expressions will be used in the sequel to obtain a geometrical description of the discretized flow.

5.1. *Coordinates near equilibria*

Let $\mathbf{v}$ and $\mathbf{w}$ stand for any of the two symmetry-related equilibria $\pm\mathbf{v}$ and $\pm\mathbf{w}$, respectively. By Samovol's theorem [24] f may be linearized around them, since non-resonance is automatic here. In cylindrical coordinates (ρ, θ, z) the linearizations take the forms:

$$\begin{cases} \dot\rho = -C_v\rho \\ \dot\theta = 1 \\ \dot z = E_v z \end{cases} \qquad \begin{cases} \dot\rho = E_w\rho \\ \dot\theta = 1 \\ \dot z = -C_w z. \end{cases} \tag{2}$$

We consider cylindrical neighbourhoods of $\mathbf{v}$ and $\mathbf{w}$ in $\mathbf{S}^3$ of radius $\varepsilon > 0$ and height 2ε. Their boundaries consist of three components (see Figure 5):

- The cylinder wall parametrized by $x \in \mathbf{R} \pmod{\mathbf{2}\pi}$ and $|y| \le \varepsilon$ with the usual cover $(x, y) \mapsto (\varepsilon, x, y) = (\rho, \theta, z)$.
- Two discs, the top and the bottom of the cylinder. We take polar coverings of these discs: $(r, \varphi) \mapsto (r, \varphi, j\varepsilon) = (\rho, \theta, z)$ where $j \in \{-, +\}$, $0 \le r \le \varepsilon$ and $\varphi \in \mathbf{R} \pmod{\mathbf{2}\pi}$.

We use x for the angular coordinate on the cylinder wall so as to avoid confusion with the angular coordinate on the discs when dealing with the local maps.

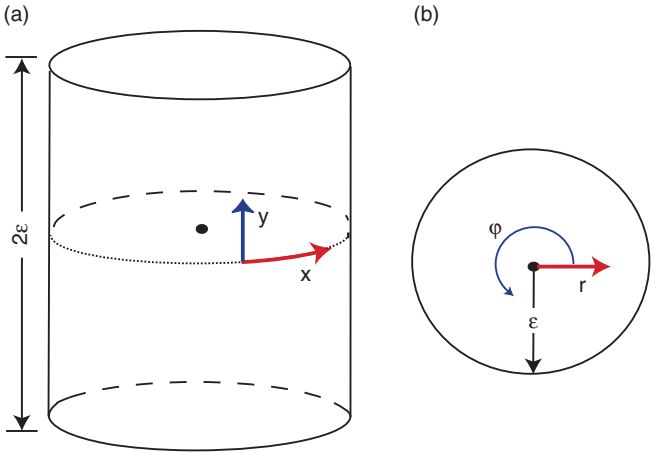

Figure 5. Coordinates on the boundaries of the neighbourhood of **v** and **w**: (a) cylinder wall (b) top and bottom.

Note that the two flows defined by (2) have symmetry $\mathbf{Z}_2 \oplus \mathbf{SO}(2)$ given by $z \mapsto -z$ and rotation around the z-axis. This is an artefact of the linearization and has nothing to do with the original symmetries. It will be used implicitly in the next sections.

5.2. *Local dynamics near v*

The cylinder wall is denoted H_v^{in}. Trajectories starting at interior points of H_v^{in} go inside the cylinder in positive time and $H_v^{\text{in}} \cap W^s(\mathbf{v})$ is parametrized by $y = 0$. The set of points in H_v^{in} with positive (respectively negative) second coordinate is denoted $H_v^{\text{in},+}$ (respectively $H_v^{\text{in},-}$).

The top and the bottom of the cylinder are denoted $H_v^{\text{out},+}$ and $H_v^{\text{out},-}$, respectively. Trajectories starting at interior points of either $H_v^{\text{out},+}$ or $H_v^{\text{out},-}$ go inside the cylinder in negative time (see Figure 6).

After linearization $W^u(\mathbf{v})$ is the z-axis, intersecting $H_v^{\text{out},+}$ at the origin of coordinates of $H_v^{\text{out},+}$. Trajectories starting at $H_v^{\text{in},j}$, $j \in \{+,-\}$ leave the cylindrical neighbourhood at $H_v^{\text{out},j}$. The orientation of the z-axis may be chosen to have $[\mathbf{v} \to j\mathbf{w}]$ meeting $H_v^{\text{out},j}$.

The local map near **v**, $\phi_v : H_v^{\text{in},+} \to H_v^{\text{out},+}$ is given by

$$\phi_v(x,y) = \left(K_v y^{\delta_v},\ -\frac{1}{E_v}\ln y + x + \frac{1}{E_v}\ln(\varepsilon) \right) = (r,\phi)\,, \tag{3}$$

where

$$\delta_v = \frac{C_v}{E_v} > 0, \quad K_v = \varepsilon^{1-\delta_v} > 0 \quad \text{and} \quad \frac{1}{E_v} > 0.$$

The expression for the local map from $H_v^{\text{in},-}$ to $H_v^{\text{out},-}$ is the same.

5.3. *Local dynamics near w*

After linearization, $W^s(\mathbf{w})$ is the z-axis, intersecting the top and bottom of the cylinder at the origin of the coordinates. We denote by $H_w^{\text{in},j}$, $j \in \{-,+\}$, the component that

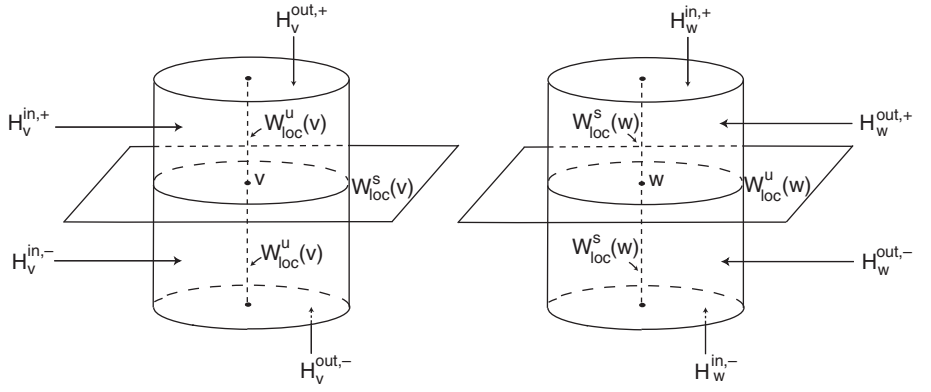

Figure 6. Neighbourhoods of the saddle-foci. Left: once the flow enters the cylinder transversely across the wall $H_v^{\text{in}} \setminus W^s_{\text{loc}}(\mathbf{v})$ leaves it transversely across the cylinder top $H_v^{\text{out},+}$ and bottom $H_v^{\text{out},-}$. Right: the flow enters the cylinder transversely across top $H_w^{\text{in},+} \setminus W^s_{\text{loc}}(\mathbf{w})$ and bottom $H_w^{\text{in},-} \setminus W^s_{\text{loc}}(\mathbf{w})$ and leaves it transversely across the wall H_w^{out}. Inside the two cylinders the vector field is linear.

$[j\mathbf{v} \to \mathbf{w}] \cap H_w^{\text{in},j} \neq \emptyset$. Trajectories starting at interior points of $H_w^{\text{in},\pm}$ go inside the cylinder in positive time (see Figure 6).

Trajectories starting at interior points of the cylinder wall H_w^{out} go inside the cylinder in negative time. The set of points in H_w^{out} whose second coordinate is positive (respectively negative) is denoted $H_w^{\text{out},+}$ (respectively $H_w^{\text{out},-}$) and $H_w^{\text{out}} \cap W^u(\mathbf{w})$ is parametrized by $y = 0$. The orientation of the z-axis may be chosen to have trajectories that start at $H_w^{\text{in},j} \setminus W^s(\mathbf{w})$, $j \in \{+,-\}$ leaving the cylindrical neighbourhood at $H_w^{\text{out},j}$. The local map near $\mathbf{w}$, $\phi_w : H_w^{\text{in},+} \setminus W^s(\mathbf{w}) \to H_w^{\text{out},+}$ is

$$\phi_w(r,\varphi) = \left(\frac{1}{E_w}\ln(\varepsilon) - \frac{1}{E_w}\ln r + \varphi, K_w r^{\delta_w}\right) = (x,y),$$

where

$$\delta_w = \frac{C_w}{E_w} > 0, \quad K_w = \varepsilon^{1-\delta_w} > 0 \quad \text{and} \quad \frac{1}{E_w} > 0.$$

The same expression holds for the local map from $H_w^{\text{in},-} \setminus W^s(\mathbf{w})$ to $H_w^{\text{out},-}$.

5.4. *Local dynamics near the closed trajectory C*

Consider a local cross section S to the flow at $p \in \mathbf{C}$. The Poincaré first return map defined on S may be linearized around the hyperbolic fixed point p using Samovol's theorem. Suspending the linear map yields, in cylindrical coordinates, the differential equations:

$$\begin{cases} \dot{\rho} = -C_C(\rho - 1) \\ \dot{\theta} = 1 \\ \dot{z} = E_C z \end{cases} \tag{4}$$

that are locally orbitally equivalent to the original flow. In these coordinates, $\mathbf{C}$ corresponds to the circle $\rho = 1$ and $z = 0$, $W^s(\mathbf{C})$ is the plane $z = 0$ and $W^u(\mathbf{C})$ is the cylinder $\rho = 1$.

We work with a hollow three-dimensional cylindrical neighbourhood of **C** with boundary $H_C^{\text{in}} \cup H_C^{\text{out}}$, where trajectories starting in H_C^{in} (respectively H_C^{out}) go into the neighbourhood in positive (respectively negative) small time. In what follows, we establish some notation for components of the boundary (see Figure 7).

The components of H_C^{in} are the two cylinder walls, $H_{C,+}^{\text{in}}$ and $H_{C,-}^{\text{in}}$ locally separated by $W^u(\mathbf{C})$ and parametrized by the covering map:

$$(x, y) \mapsto (1 \pm \varepsilon, x, y) = (\rho, \theta, z),$$

where $x \in \mathbf{R} \pmod{2\pi}$, $|y| < \varepsilon$. We denote by $H_{C,+}^{\text{in}}$ the component with $\rho = 1 + \varepsilon$.

In these coordinates, $H_C^{\text{in}} \cap W^s(\mathbf{C})$ is the union of the two circles $y = 0$ in the two components. It divides $H_{C,+}^{\text{in}}$ in two parts, $H_{C,+}^{\text{in},+}$ and $H_{C,+}^{\text{in},-}$, parametrized, respectively, by positive and negative y, with a similar convention for $H_{C,-}^{\text{in},+}$ and $H_{C,-}^{\text{in},-}$.

The components $H_C^{\text{out},+}$ and $H_C^{\text{out},-}$ of H_C^{out} are two annuli, locally separated by $W^s(\mathbf{C})$ and parametrized by the covering:

$$(r, \varphi) \mapsto (r, \varphi, \pm\varepsilon) = (\rho, \theta, z),$$

for $1 - \varepsilon < r < 1 + \varepsilon$ and $\varphi \in \mathbf{R} \pmod{2\pi}$ and where $H_C^{\text{out},+}$ is the component corresponding to the + sign and $H_C^{\text{out}} \cap W^u(\mathbf{C})$ is the union of two circles parametrized by $r = 1$.

Denote by $H_{C,+}^{\text{out},k}$ (respectively $H_{C,-}^{\text{out},k}$), $k \in \{+, -\}$ the set parametrized by $1 < r < 1 + \varepsilon$ (respectively $1 - \varepsilon < r < 1$) in $H_C^{\text{out},k}$. In these coordinates the local map $\phi_C : H_{C,j}^{\text{in},k} \to H_{C,j}^{\text{out},k}$, $j, k \in \{+, -\}$, is given by

$$\phi_C(x, y) = \left(jK_c y^{\delta_c} + 1, \frac{1}{E_c} \ln(\varepsilon) - \frac{1}{E_c} \ln y + x \right) = (r, \varphi),$$

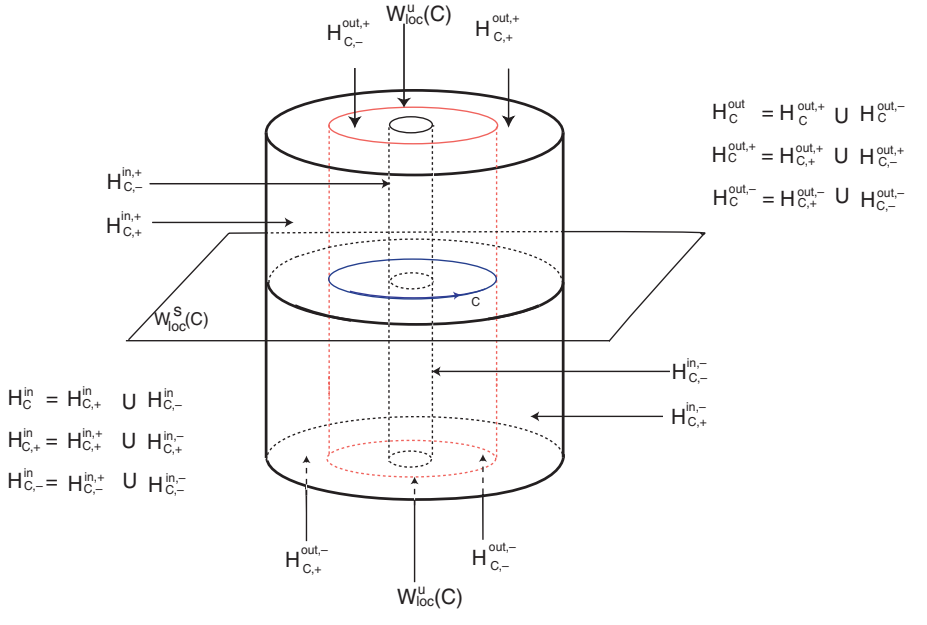

Figure 7. Neighbourhood of the closed trajectory **C**. The flow enters the hollow cylinder transversely across cylinder walls $H_{C,\pm}^{\text{in}}$ and leaves it transversely across top $H_{C,+}^{\text{out}}$ and bottom $H_{C,-}^{\text{out}}$.

where

$$\delta_c = \frac{C_c}{E_c} > 0, \quad K_c = \varepsilon^{1-\delta_C} > 0, \quad \text{and} \quad \frac{1}{E_c} > 0.$$

6. Geometry near the saddles

The coordinates and notation of Section 5 may now be used to analyse the geometry of the local dynamics near each saddle. The manifold $W^s(\mathbf{v})$ separates the cylindrical neighbourhood of $\mathbf{v}$ into an upper and a lower component, mapped into neighbourhoods of $+\mathbf{w}$ and $-\mathbf{w}$, respectively. We show here that initial conditions lying on a segment on the upper part of the cylindrical wall around $\mathbf{v}$ and ending at $W^s(\mathbf{v})$ are mapped into points on a spiral on the top of the cylinder H_v^{out} where the flow goes out (Figure 8).

Initial conditions on a spiral on the top of cylindrical neighbourhood of $\mathbf{w}$ are then shown to be mapped into points on a helix around the cylinder accumulating on $W^u(\mathbf{w})$ (Figure 8). Since $W^s(\mathbf{C})$ is transverse to $W^u(\mathbf{w})$, then the helix on $H_w^{\text{out},+}$ is mapped across $W^s(\mathbf{C})$ on H_C^{in} infinitely many times. This is used in Section 7 to obtain, in any segment on $H_v^{\text{in},+}$, infinitely many intervals that are mapped into segments on H_C^{in} ending at $W^s(\mathbf{C})$.

Then the image of a segment ending at $W^s(\mathbf{C})$ on one of the walls of H_C^{in} is shown to be mapped into a curve accumulating on $W^u(\mathbf{C}) \cap H_C^{\text{out}}$ (see Figure 9). This curve meets $W^s(\mathbf{v})$ infinitely many times by transversality and it is thus mapped across $W^s(\mathbf{v})$ on H_v^{in} infinitely many times. Again, we use this in Section 7 to obtain infinitely many intervals that are mapped into segments on H_v^{in} ending at $W^s(\mathbf{v})$.

This structure of segments containing intervals that are successively mapped into segments allows us to establish a recurrence in Section 8 and to construct nested sequences of intervals containing the initial conditions for switching.

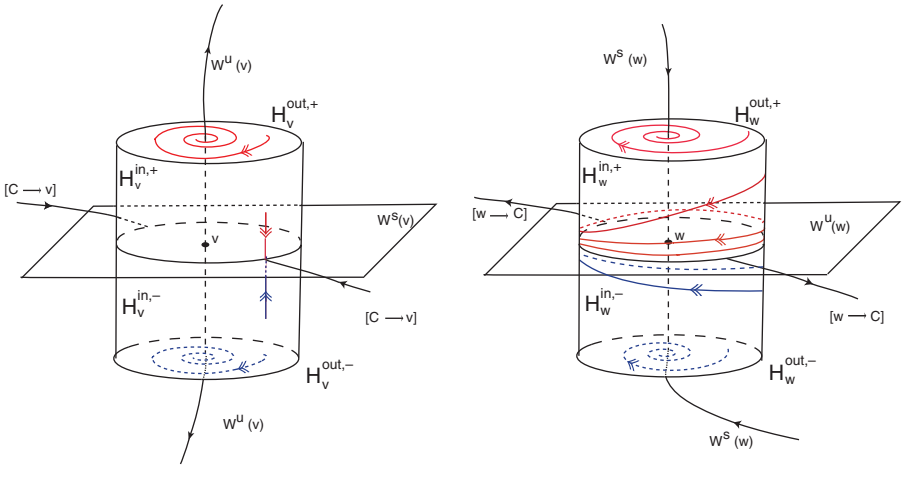

Figure 8. Local dynamics near the saddle-foci. Left: near $\mathbf{v}$, any segment on the cylinder wall is mapped into a spiral on the top or bottom of the cylinder. Right: a spiral on the top or bottom of the cylinder near $\mathbf{w}$ is mapped into a helix on the cylinder wall accumulating on $W^u(\mathbf{w})$. The double arrows on the segment, spiral and helix indicate correspondence of orientation and not the flow.

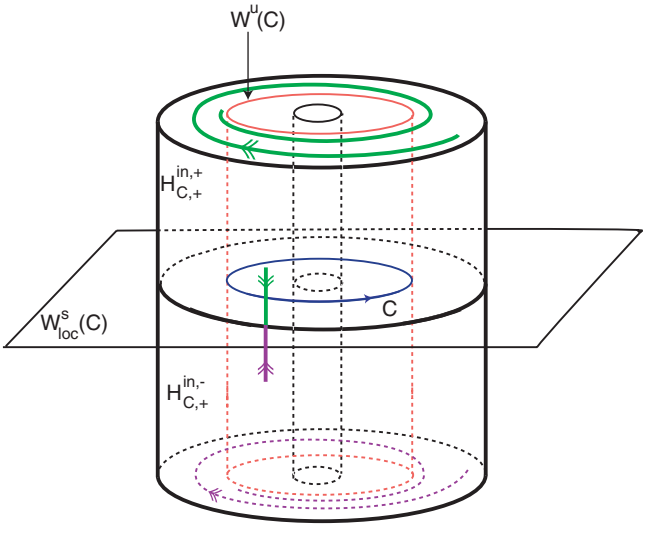

Figure 9. Local dynamics near the closed trajectory **C**. A segment on the wall ending at $W^s(\mathbf{C})$ is mapped into a curve accumulating on $W^u(\mathbf{C}) \cap H_C^{\text{out}}$.

Definition 1: A segment β on H_v^{in} (respectively: H_C^{in}) is a smooth regular parametrized curve $\beta : [0, 1] \to H_p^{\text{in}}$ (respectively: $\beta : [0, 1] \to H_C^{\text{in}}$) that meets $W^s(\mathbf{v})$ (respectively $W^s(\mathbf{C})$) transversely at the point $\beta(1)$ only and such that, writing $\beta(s) = (x(s), y(s))$, both x and y are monotonic functions of s.

The coordinates (x, y) may be chosen so as to make the angular coordinate x an increasing or decreasing function of s as convenient.

Definition 2: Let U be an open set in a plane in $\mathbf{R}^n$ and $p \in U$. A spiral on U around p is a curve $\alpha : [0, 1) \to U$ satisfying $\lim_{s\to 1^-} \alpha(s) = p$ and such that, if $\alpha(s) = (\alpha_1(s), \alpha_2(s))$ are its expressions in polar coordinates (ρ, θ) around p, then α_1 and α_2 are monotonic with

$$\lim_{s\to 1^-} |\alpha_2(s)| = +\infty.$$

It follows that α_1 is a decreasing function of s.

Proposition 1: *A segment β on $H_v^{\text{in},+}$ (respectively $H_v^{\text{in},-}$) is mapped by ϕ_v into a spiral on $H_v^{\text{out},+}$ (respectively $H_v^{\text{out},-}$) around $W^u(\mathbf{v})$.*

Proof: Write $\beta(s) = (x(s), y(s))$ on $H_v^{\text{in},+}$ with $y(s) \geq 0$ monotonically decreasing and choose a parametrization of $H_v^{\text{in},+}$ such that $x(s)$ is monotonically increasing. Then, writing $\phi_v(\beta(s)) = (r(s), \theta(s))$, it follows from the expression of ϕ_v in Section 5.2 that $r(s)$ is monotonically decreasing while $\theta(s)$ is monotonically increasing. From $\lim_{s\to 1^-} y(s) = 0$ and $\lim_{s\to 1^-} x(s) = x(1)$ the required limits $\lim_{s\to 1^-} r(s) = 0$ and $\lim_{s\to 1^-} \theta(s) = +\infty$ follow. □

Definition 3: Let $a, b \in \mathbf{R}$ such that $a < b$ and let H be a surface parametrized by a cover $(\theta, h) \in \mathbf{R} \times [a, b]$ where θ is periodic. *A helix on H accumulating on the circle $h = h_0$* is a curve $\gamma : [0, 1) \to H$ such that its coordinates $(\theta(s), h(s))$ are monotonic functions of s with

$$\lim_{s\to 1^-} h(s) = h_0 \quad \text{and} \quad \lim_{s\to 1^-} |\theta(s)| = +\infty.$$

Proposition 2: *A spiral on $H_w^{\text{in},+}$ (respectively $H_w^{\text{in},-}$) around $W^s(\mathbf{w})$ is mapped by ϕ_w into a helix on $H_w^{\text{out},+}$ (respectively $H_w^{\text{out},-}$) accumulating on the circle $H_w^{\text{out}} \cap W^u(\mathbf{w})$.*

Proof: Parametrize $H_w^{\text{in},+}$ so that a spiral $\sigma(s) = (r(s), \theta(s))$ around $W^s(\mathbf{w})$ has $\theta(s)$ increasing with s. The expression of ϕ_w of Section 5.3 ensures that in $\phi_w(\sigma(s)) = (x(s), y(s))$ we have y decreasing with s and x increasing with s. The limits in the definition of helix follow from the form of ϕ_w and from $\lim_{s\to 1^-} r(s) = 0$ and $\lim_{s\to 1^-} \theta(s) = +\infty$. □

Proposition 3: *A segment β on $H_{C,+}^{\text{in},+}$ is mapped by ϕ_C into a helix on $H_{C,+}^{\text{out},+}$ accumulating on the circle $W^u(\mathbf{C}) \cap H_C^{\text{out},+}$.*

The proof, as in Propositions 1 and 2, consists of using the expression of ϕ_C of Section 5.4 after a suitable choice of orientation in $H_{C,+}^{\text{in},+}$. Using the symmetries of the linearized flow, it follows that Proposition 3 also holds for a segment β on $H_{C-}^{\text{in},+}$ and for $H_{C-}^{\text{out},+}$, as well as for a segment β on $H_{C+}^{\text{in},-}$ and for $H_{C+}^{\text{out},-}$ and for β on $H_{C-}^{\text{in},-}$ and for $H_{C-}^{\text{out},-}$, considering the circle $W^u(\mathbf{C}) \cap H_C^{\text{out},-}$ (see Figure 9).

7. First return to v

Let p and q be two nodes of Σ such that there is a connection $[p \to q]$. The transition map $\Psi_{p,q}$ from H_p^{out} to H_q^{in} follows the trajectory $[p \to q]$ in flow-box fashion. In this section, we use this information to put together the local behaviour of trajectories that start near $\pm\mathbf{v}$. To simplify the reading, we omit the $-$ and $+$ signs.

Let $P \in H_w^{\text{out}}$ be one of the points where $[\mathbf{w} \to \mathbf{C}]$ meets H_w^{out}. For small a, $b > 0$, the rectangle $[-\frac{a}{2}, \frac{a}{2}] \times [-\frac{b}{2}, \frac{b}{2}]$ is mapped diffeomorphically into H_w^{out} by the parametrization that maps the origin to P (Figure 10). Its image, that we denote by R_w, will be called a *rectangle in H_w^{out} centred at P* with *height b*.

The *vertical sides* of R_w are the images of the segments $(\pm\frac{a}{2}, y)$ with $y \in [-\frac{b}{2}, \frac{b}{2}]$. Rectangles in H_C^{out} centred at a given point are defined in the same way; we denote them by R_C.

By Propositions 1 and 3, the map

$$\eta = \phi_w \circ \Psi_{v,w} \circ \phi_v : H_v^{\text{in}} \to H_w^{\text{out}}$$

maps a segment β on H_v^{in} infinitely many times across any small rectangle in H_w^{out} centred at a point in $W^u(\mathbf{w})$.

An *admissible family of intervals* $\mathcal{I} = \{[a_i, b_i]\}_{i\in\mathbf{N}}$ is one that satisfies

$$0 < a_i < b_i < a_{i+1} < 1 \quad \text{and} \quad \lim_{i\to\infty} a_i = 1.$$

Proposition 4: *Let R_w be a rectangle in H_w^{out} centered at one point P of $H_w^{\text{out}} \cap [\mathbf{w} \to \mathbf{C}]$. For any segment $\beta : [0,1] \longrightarrow H_v^{\text{in}}$ there is an admissible family of intervals $\{[\sigma_i, \rho_i]\}_{i\in\mathbf{N}}$ such that*

(1) *each closed interval $[\sigma_i, \rho_i]$ satisfies $\eta \circ \beta([\sigma_i, \rho_i]) \subset R_w$;*
(2) *each open interval (ρ_{i+1}, σ_i) satisfies $\eta \circ \beta((\rho_{i+1}, \sigma_i)) \cap R_w = \emptyset$ and*
(3) *the family of curves $\{\eta \circ \beta([\sigma_i, \rho_i])\}$ accumulates uniformly on $W^u(\mathbf{w}) \cap R_w$ as $i \to +\infty$.*

This also holds for the local map around **C**, *with* **C**, ϕ_C *and* **C** *where we have written* **w**, η *and* **v**.

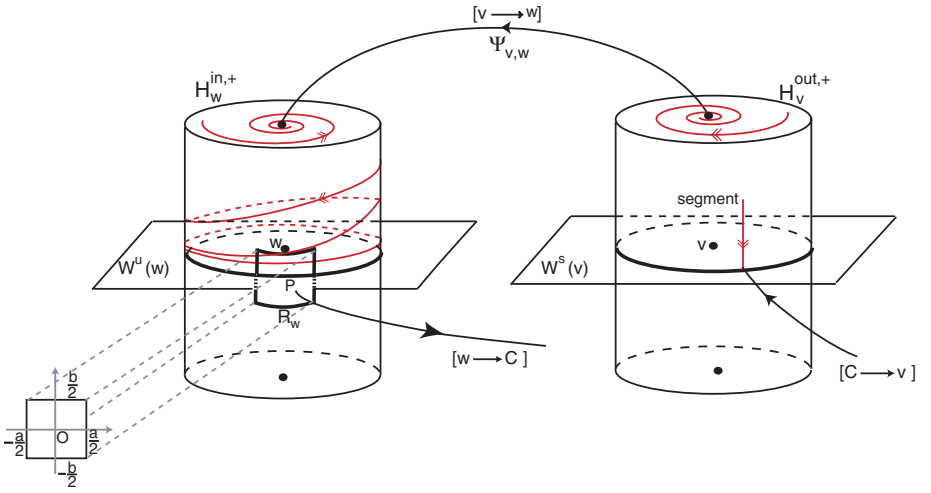

Figure 10. Transition from **v** to **w**: a segment on H_v^{in} is mapped into spirals on H_v^{out} around $W^u(\mathbf{v}) \cap H_v^{\text{out}}$ and $W^s(\mathbf{w}) \cap H_w^{\text{in}}$. The spiral is then mapped into a helix on H_w^{out} accumulating on $W^u(\mathbf{w})$ and crossing infinitely many times a rectangle R_w centred at one of the connections starting at **w** (see also Figure 11). Double arrows indicate orientation of the segment and not the flow.

Proof: Writing $(x(s), y(s))$ for the coordinates of the helix $\eta \circ \beta(s)$ on the cylinder wall, we have that y decreases with s and that $x(s)$ can be taken as an increasing function of s by choosing compatible orientations in H_v^{in} and H_w^{out} and, if necessary, by restricting the domain of β to a smaller interval $(s_1, 1)$. In particular, the helix $\eta \circ \beta$ may be seen as a graph $(x, y(x))$ where $x \in [x(0), +\infty)$ and where y is a decreasing function of x with $\lim_{x\to\infty} y(x) = 0$ (Figure 11).

On H_w^{out}, the rectangle R_w is $[n - a/2, n + a/2] \times [-b/2, b/2]$ with $n \in \mathbf{N}$. Let σ_0 be the smallest value of $s \in (s_1, 1)$ such that $(x(s), y(s))$ lies on the left-vertical side of R_w, with $y(\sigma_0) < \frac{b}{2}$ as in Figure 11. Then $y(s) < \frac{b}{2}$ for all $s \in [\sigma_0, 1)$.

The sequences defining the family of intervals are obtained from points where the helix meets successive copies of the vertical sides of R_w with $x(\sigma_i) = n_0 + i - a/2$ and $x(\rho_i) = n_0 + i + a/2$. The proof for ϕ_C is similar. □

Proposition 5: *Given a segment* $\beta : [0, 1] \longrightarrow H_v^{\text{in}}$, *a rectangle* R_w *of sufficiently small height and the family of intervals* $\{[\sigma_i, \rho_i]\}_{i\in\mathbf{N}}$ *of Proposition* 4. *Then for sufficiently large i there are* τ_i *with* $\sigma_i < \tau_i < \rho_i$ *such that* $\Psi_{w,C} \circ \eta(\beta(\tau_i)) \in W^s(\mathbf{C})$ *and* $\Psi_{w,C} \circ \eta \circ \beta$ *maps each one of the intervals* $[\sigma_i, \tau_i]$ *and* $[\tau_i, \rho_i]$ *into a segment on one of the sets* $H_C^{\text{in},+}$ *and* $H_C^{\text{in},-}$. *This also holds for* $\Psi_{C,v} \circ \phi_C : H_C^{\text{in}} \longrightarrow H_v^{\text{in},\pm}$ *with the appropriate changes.*

Proof: Since $W^s(\mathbf{C}) \cap H_w^{\text{out}}$ meets $W^u(\mathbf{w}) \cap \mathbf{H}_{\mathbf{w}}^{\text{out}}$ transversely (property (P5)) then if the height of R_w is small, $W^s(\mathbf{C})$ does not meet its vertical sides. Each one of the images $\eta \circ \beta([\sigma_i, \rho_i])$ meets $W^s(\mathbf{C}) \cap H_w^{\text{out}}$ transversely at a single point $\eta \circ \beta(\tau_i)$, since they accumulate uniformly on $W^u(\mathbf{w}) \cap R_w$ as $i \to +\infty$. The monotonicity of the coordinates of $\eta \circ \beta$ will be preserved by $\Psi_{w,C}$ close to $W^u(\mathbf{w})$. Each component of $\eta \circ \beta([\sigma_i, \rho_i]) \setminus \{\eta \circ \beta(\tau_i)\}$ will be mapped into a segment, one into each connected component of $H_C^{\text{in},j} \setminus W^s(\mathbf{C})$. The proof for $\Psi_{C,v} \circ \phi_C$ is analogous. □

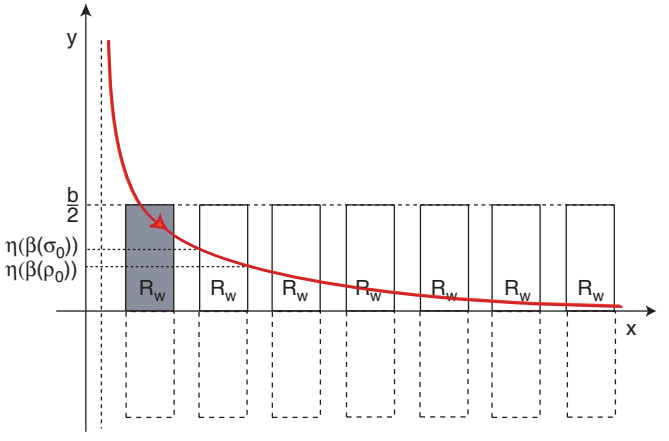

Figure 11. A helix on a periodic cover of the cylinder wall H_w^{out}. After it meets the first (shaded) copy of the rectangle, the helix will intersect the rectangle at intervals whose image accumulates on the curve $W^u(\mathbf{w})$, represented here by the x-axis.

8. Switching near the heteroclinic network

In this section, we put together the information about the first return map to H_v^{in}. In Sections 6 and 7, we have found that a segment ending at the stable manifold of one node contains intervals that are mapped into segments ending at the stable manifold of the next node. Starting with a segment on H_v^{in}, here this is used recursively to obtain sequences of nested intervals containing initial conditions that follow sequences of heteroclinic connections.

We say that the path $s^k = (c_j)_{j\in\{1,\ldots,k\}}$ of order k on the network Σ is *inside* the path $t^{k+l} = (d_j)_{j\in\{1,\ldots,k+l\}}$ of order $k+l$ (denoted $s^k \prec t^{k+l}$) if $c_j = d_j$ for all $j \in \{1,\ldots,k\}$.

The family of closed intervals $\mathcal{I} = \{I_i\}_{i\in\mathbf{N}}$ is *inside* the family $\tilde{\mathcal{I}} = \{\tilde{I}_i\}_{i\in\mathbf{N}} (\mathcal{I} \prec \tilde{\mathcal{I}})$ if, for all $i \in \mathbf{N}$, $I_i \subset \tilde{I}_i$. If $\tilde{\mathcal{I}}$ is admissible in the sense of Section 7 and $\mathcal{I} \prec \tilde{\mathcal{I}}$ then $\mathcal{I}$ is also admissible, provided none of its intervals consists of a point.

Theorem 6: *There is finite switching near the network Σ defined by a vector field satisfying (P1–P5).*

Proof: Given a path, we want to find trajectories that follow it into the neighbourhoods of Section 5 going through small discs in H_v^{out} around $W^u(\pm\mathbf{v})$ and through rectangles in H_w^{out} and H_C^{out} centred at the connections. Without loss of generality we only consider paths $s^k = (c_j)_{j\in\{1,\ldots,k\}}$ starting with $c_1 = [\pm\mathbf{v} \to \pm\mathbf{w}]$.

Take a segment β on $H_v^{\text{in},\pm}$ of points that follow the first connection c_1. We will construct admissible families of intervals $\mathcal{I}(c_1,\ldots,c_n) = \{I_i\}_{i\in\mathbf{N}}$ recursively, such that points in $\beta(I_i)$ follow $(c_1,\ldots,c_n)$ and the image of $\beta(I_i)$ by the transition maps is a segment (see Figure 12). We will show that $s^k \prec s^{k+l}$ implies $\mathcal{I}(s^k) > \mathcal{I}(s^{k+l})$ and thus the process will be recursive.

By Propositions 4 and 5, there is an admissible family of intervals $\mathcal{I}(c_1,c_2) = \{I_i\}_{i\in\mathbf{N}}$ such that $\beta(I_i)$ is mapped by $\Psi_{w,C} \circ \phi_w \circ \Psi_{v,w} \circ \phi_v$ into a segment on $H_C^{\text{in},\pm}$ with the choice of sign appropriate for the next connection c_3. Applying the second part of Propositions 4 and 5 to this segment, we obtain an admissible family of intervals $\mathcal{I}(c_1,c_2,c_3) < \mathcal{I}(c_1,c_2)$ corresponding to points that follow (c_1,c_2,c_3) and to intervals that are mapped into a segment on $H_v^{\text{in},\pm}$ with the choice of sign appropriate for following the connection c_4.

In Proposition 5 we assume the height of the rectangle R_w is small and we reduce it if necessary. This is done to ensure that inside R_w the stable manifold $W^s(\mathbf{C})$ is the graph of a function and thus a helix only meets it once at each turn. However, as soon as the choice of height is made it may be kept throughout the proof and thus the construction of $\mathcal{I}(s^k)$ is recursive, proving finite switching near Σ. □

Theorem 7: *There is infinite switching near the network* Σ *defined by a vector field satisfying* (*P1–P5*).

Proof: Fix an infinite path $s^\infty = (c_j)_{j\in\mathbf{N}}$ on Σ. For each $k \in \mathbf{N}$ define the finite path s^k of order k by $s^k = (c_j)_{j\in\{1,\ldots,k\}}$, with $s^k < s^{k+1}$. From the proof of Theorem 6, for each k we have an admissible family of intervals $\mathcal{I}(s^k) = \{J_{ki}\}_{i\in\mathbf{N}}$ such that $\mathcal{I}(s^k) > \mathcal{I}(s^{k+1})$ and all the points in $\beta(J_{ki})$ follow s^k.

Since we have $\mathcal{I}(s^k) > \mathcal{I}(s^{k+1})$ then $\Lambda = \cap_{k=1}^{\infty}\mathcal{I}(s^k)$ is non-empty because each set $\Lambda_i = \cap_{k=1}^{\infty} J_{ki}$ is non-empty. From the definition of admissible family of intervals, if we take $a_i \in \Lambda_i$ then $\lim_{i\to\infty} a_i = 1$. From the construction we have that $\beta(a_i)$ follows s^∞. Thus, we have obtained a sequence of points $\beta(a_i)$ that accumulate on Σ as $i \to \infty$ and that follow the infinite path. □

9. Final remarks and discussion

9.1. *Generalization*

Not all assumptions of Section 3 are essential to prove switching, although some of them simplify the calculations. For instance, the eigenvalues at $\pm\mathbf{v}$ and $\pm\mathbf{w}$ may have any imaginary part, not necessarily 1 as in (P3). The proof also works if at one of the pairs of nodes $\pm\mathbf{v}$ or $\pm\mathbf{w}$ the eigenvalues of df are real, as long as the eigenvalues at the other pair of nodes are not real – it is enough to have one pair of rotating equilibria. Any finite number of one-dimensional connections $[\mathbf{w} \to \mathbf{C}]$ and $[\mathbf{C} \to \mathbf{v}]$ could have been used instead of two for each equilibrium.

The existence of switching near a network may be easily generalized to a heteroclinic network involving any number of rotating nodes such that each heteroclinic connection involving a periodic trajectory is transverse and there are no consecutive non-transverse heteroclinic connections on the network.

It is not essential to have $(\mathbf{Z}_2 \oplus \mathbf{Z}_2)$-equivariance. The symmetry γ_2 is used here to obtain the closed trajectory $\mathbf{C}$ and the role of γ_1 is to guarantee that the one-dimensional connections $[\mathbf{v} \to \mathbf{w}]$ are robust. Symmetries make the existence of the network natural and ensure persistence. Switching will hold for any network without symmetry having the nodes and connections prescribed here, as long as the remaining assumptions are satisfied.

Estimates for the transition maps may be refined as in Aguiar *et al.* [16] to show that near this network there is a suspended horseshoe with transition map described as a full shift over a countable set of symbols. The suspended horseshoe has the same shape as the network. Thus, when the symmetry of the example in Section 4, is partly broken we have instant chaos. In particular, it can be shown that there are periodic orbits that follow any finite path in the network, but this uses techniques beyond the scope of this article.

Finite switching is present even when all the local maps are expanding, as in the case $C_v < E_v$, $C_w < E_w$, $C_C < E_C$. This is due to the rotation around the nodes and is markedly different from the situation where all eigenvalues are real. In the example of Section 4, this corresponds to parameter values where the $\mathbf{O}(2)$-symmetric network is a repeller.

A path on the network can also be shadowed by trajectories in $W^u(\mathbf{C})$ (see Figure 12) because the local unstable manifold of $\mathbf{C}$ meets H_v^{in} at a segment by the transversality assumption (P5). It also follows that there are infinitely many homoclinic connections involving the periodic trajectory $\mathbf{C}$, although there are no homoclinic trajectories involving the equilibria. The geometry of $W^u(\mathbf{C})$ gets extremely complicated as we move away from $\mathbf{C}$, since it will accumulate on the whole network, having $\mathbf{v}$, $\mathbf{w}$ and $\mathbf{C}$ as limit points. A complete description of the non-wandering set for this type of flows is in preparation.

9.2. *Discussion*

Generic breaking of the γ_1-symmetry destroys the network, as in [17,18], by breaking the connections $[\mathbf{v} \to \mathbf{w}]$. If the remaining assumptions are still satisfied, a weaker form of switching will hold: for small symmetry-breaking terms, it may still be possible to find trajectories that visit neighbourhoods of finite sequences of nodes. This is because the spirals on top of the cylinder around $\mathbf{w}$ of Figure 8 will be off-centred and will turn a finite number of times around $W^s(\mathbf{w})$. From this we may obtain points whose trajectories follow short finite paths on the network. As $W^u(\mathbf{v})$ gets closer to $W^s(\mathbf{w})$ (as the system moves closer to symmetry) the paths that can be shadowed get longer.

This is in contrast to the findings of Kirk and Rucklidge [18], who claim that there can be no switching in generic systems close to the symmetric case, so a comparison of the settings and results of the two papers is in order at this point. The first caveat is that the $\mathbf{Z}_2 \oplus \mathbf{Z}_2$ representations are different: in our case $\text{Fix}(\mathbf{Z}_2 \oplus \mathbf{Z}_2) = \{0\}$, and there are two transverse two-dimensional fixed-point subspaces for the isotropy subgroups, whereas in [18], $\text{Fix}(\mathbf{Z}_2 \oplus \mathbf{Z}_2)$ is a plane with two one-dimensional fixed-point subspaces for the isotropy subgroups. In their setting, our symmetries correspond to the group generated by a rotation of π in $\mathbf{SO}(2)$ and by the product of their $\mathbf{Z}_2 \oplus \mathbf{Z}_2$ generators. Both representations occur in the larger group $\mathbf{Z}_2 \oplus \mathbf{Z}_2 \oplus \mathbf{SO}(2)$ used in [17]. Moreover, we are assuming the existence of an invariant three-sphere (a natural assumption in the symmetric context, see [1]) and it is not evident that in their context such a sphere will exist.

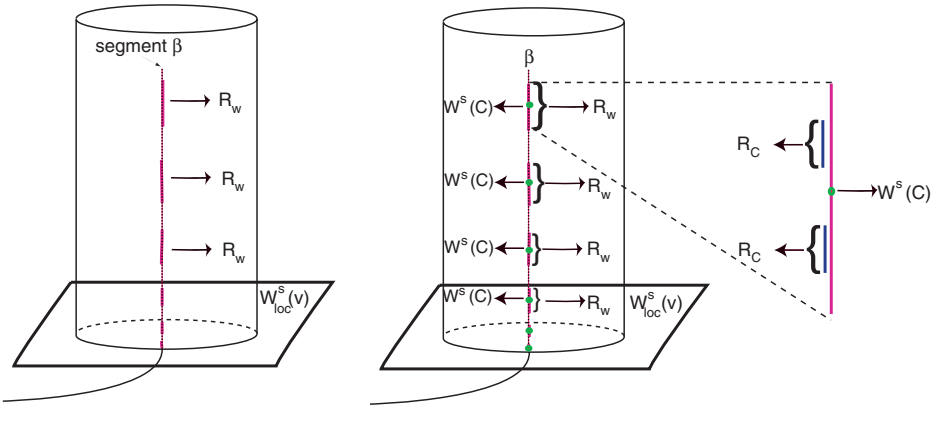

Figure 12. On a segment β on H_v^{in}, there are infinitely many small segments that are mapped by η into R_w, each one containing a point mapped into $W^s_{\text{loc}}(\mathbf{C})$. The small segments contain smaller ones that are mapped into R_C and this may be continued, forming a nested sequence.

However, the difference in the results of [18] and ours indicates that vector fields with $\mathbf{Z}_2 \oplus \mathbf{Z}_2 \oplus \mathbf{SO}(2)$ symmetry have codimension higher than three in the universe of general vector fields. This will mean that in general systems close to symmetry what will be observed may depend on the way symmetries are broken and that a lot more needs to be done before switching is well understood.

Acknowledgements

The research of all authors at Centro de Matemática da Universidade do Porto (CMUP) was financially support by Fundação para a Ciência e a Tecnologia (FCT), Portugal, through the programmes POCTI and POSI with European Union and national funding. A.A.P. Rodrigues was supported by the grant SFRH/BD/28936/2006 of FCT.

References

[1] M. Field, *Lectures on Bifurcations, Dynamics and Symmetry*, Pitman Research Notes in Mathematics Series, Vol. 356, Longman, Harlow, UK, 1996.
[2] M. Krupa, *Robust heteroclinic cycles*, J. Nonlin. Sci. 7 (1997), pp. 129–176.
[3] P. Ashwin and M. Field, *Heteroclinic networks in coupled cell systems*, Arch. Ration. Mech. Anal. 148 (1999), pp. 107–143.
[4] M. Aguiar, P. Ashwin, A. Dias, and M. Field, *Robust heteroclinic cycles in coupled cell systems: Identical cells with asymmetric inputs*, CMUP preprint 2008-06 (http://cmup.fc.up.pt/cmup/v2/frames/publications.htm).
[5] J. Hofbauer, *Heteroclinic cycles on the simplex*, Proceedings of the International Conference on Nonlinear Oscillations, Janos Bolyai Mathematical Society Budapest, 1987.
[6] J. Hofbauer and K. Sigmund, *The Theory of Evolution and Dynamical Systems*, Cambridge University Press, Cambridge, 1988.
[7] J. Hofbauer, *Heteroclinic cycles in ecological differential equations*, Tatra Mountains Math. Publ. 4 (1994), pp. 105–116.
[8] W. Brannath, *Heteroclinic networks on the tetrahedron*, Nonlinearity 7 (1994), pp. 1367–1384.
[9] J. Guckenheimer and P. Worfolk, *Instant chaos*, Nonlinearity 5 (1992), pp. 1211–1222.
[10] D. Armbruster, E. Stone, and V. Kirk, *Noisy heteroclinic networks*, Chaos 13(1) (2003), pp. 71–79.
[11] Y. Sato, E. Akiyama, and J.P. Crutchfield, *Stability and diversity in collective adaptation*, Physica D 210 (2005), pp. 21–57.
[12] I. Melbourne, *An example of a non-asymptotically stable attractor*, Nonlinearity 4 (1991), pp. 835–844.
[13] T. Ura, *On the flow outside a closed invariant set: stability, relative stability and saddle sets*, Contrib. Diff. Eqns III(3) (1964), pp. 249–94.
[14] C.M. Postlethwaite and J.H.P. Dawes, *Regular and irregular cycling near a heteroclinic network*, Nonlinearity 18 (2005), pp. 1477–1509.
[15] V. Kirk and M. Silber, *A competition between heteroclinic cycles*, Nonlinearity 7 (1994), pp. 1605–1621.
[16] M. Aguiar, S.B. Castro, and I.S. Labouriau, *Dynamics near a heteroclinic network*, Nonlinearity 18 (2005), pp. 391–414.
[17] I. Melbourne, M.R.E. Proctor, and A.M. Rucklidge, *A heteroclinic model of geodynamo reversals and excursions*, in *Dynamo and Dynamics*, A Mathematical Challenge, P. Chossat, D. Armbruster, and I. Oprea, eds., Kluwer, Dordrecht, 2001, pp. 363–370.

[18] V. Kirk and A.M. Rucklidge, *The effect of symmetry breaking on the dynamics near a structurally stable heteroclinic cycle between equilibria and a periodic orbit*, Dyn. Syst. Int. J. 23 (2008), pp. 43–74.
[19] M.I. Golubitsky, I. Stewart, and D.G. Schaeffer, *Singularities and Groups in Bifurcation Theory*, Vol. II, Springer, Berlin, 2000.
[20] M. Aguiar, *Vector fields with heteroclinic networks*, Ph.D. thesis, Departamento de Matemática Aplicada, Faculdade de Ciências da Universidade do Porto, 2003.
[21] M. Aguiar, S.B. Castro, and I.S. Labouriau, *Simple vector fields with complex behaviour*, Int. J. Bifur. Chaos 16(2) (2006), pp. 369–381.
[22] M. Krupa and I. Melbourne, *Asymptotic stability of heteroclinic cycles in systems with symmetry*, Ergodic Theory Dyn. Syst. 15 (1995), pp. 121–147.
[23] M. Krupa and I. Melbourne, *Asymptotic stability of heteroclinic cycles in systems with symmetry: II*, Proc. Roy. Soc. Edinb. 134A (2004), pp. 1177–1197.
[24] V.S. Samovol, *Linearization of a system of differential equations in the neighbourhood of a singular point*, Sov. Math. Dokl 13 (1972), pp. 1255–1959.